

Modelling Water Quality in the Elbe and its Estuary – Large Scale and Long Term Applications with Focus on the Oxygen Budget of the Estuary

Andreas Schöl, Birte Hein, Jens Wyrwa and Volker Kirchesh

Summary

The current status of numerical water quality modelling of the German part of the Elbe and its estuary (km 0 to 727) with the model QSim is presented and simulation results are compared with field data for validation. Based on a large scale 1d approach, a consistent input signal from the river (upper 585 km) is generated to investigate the context between phytoplankton development and oxygen deficits in the estuary with enhanced mean water depth (> 10 m). In the shallow and eutrophic river, phytoplankton biomass is produced up to a seasonal mean (May-October 2006) of nearly 150 $\mu\text{g chl a l}^{-1}$ causing oxygen supersaturation. In the freshwater part of the estuary, the algae biomass declines sharply and oxygen deficits occur. Our simulations demonstrate that net algae growth rates become negative due to light limitation, while high grazing losses by zooplankton (seasonal mean of 0.5 per day) causes a decline of the biomass. Due to the input of algal derived and easily degradable organic carbon imported from the river and organic carbon from algal die-off, the Elbe Estuary becomes heterotrophic and depleted of oxygen in summer.

Referring to the large scale 1d approach, we simulate and validate the long term development of the water temperature, phytoplankton, and oxygen of the Elbe Estuary for a 13-year period (1998-2010). Recent developmental steps towards more-dimensional water quality modelling with QSim by offline coupling with a hydrodynamic model are outlined. This approach is tested concerning the horizontal water temperature distribution of a side channel system of the estuary.

Keywords

water quality model, Elbe Estuary, water temperature, oxygen, phytoplankton

Zusammenfassung

Das eindimensionale Gewässergütemodell QSim wird für die deutsche Elbe einschließlich ihres Ästuars (km 0 bis 727) angewendet. Durch den Vergleich von Simulations- und Messergebnissen wird eine Validierung für das Modell gezeigt. Mit der Berechnung der Gewässergüte für den 585 km langen Flusslauf der Elbe wird ein konsistentes Eingangssignal für das Ästuar erzeugt, um damit den Sauerstoffhaushalt und die Entwicklung des Phytoplanktons im Bereich des Hamburger Hafens und der Seeschiffahrtsstraße mit seinen großen mittleren Wassertiefen (> 10 m) zu modellieren. Die Simulationen für das Jahr 2006 zeigen, dass in der Vegetationsperiode von Mai bis Oktober hohe Algenbiomassen von im Mittel etwa 150 $\mu\text{g chl a l}^{-1}$ im flachen und eutrophen Flussabschnitt der Elbe produziert werden. Diese hohe Primärproduktion führt auch zu deutlichen Sauerstoffübersättigungen auf der Fließstrecke. Im anschließenden limnischen Abschnitt des Elbe-Ästuars geben dann die Algengehalte deutlich zurück. Parallel

dazu treten Sauerstoffdefizite auf. Die Analyse der Modellergebnisse bezüglich des Rückgangs der Algen zeigt, dass das netto-Algenwachstum in den tiefen Abschnitten des Ästuars aufgrund der Lichtlimitierung negative Raten annimmt und gleichzeitig starke Verluste durch den Wegfraß durch das Zooplankton (Saisonmittel von 0.5 pro Tag) auftreten. Der Eintrag von lebenden Algen und leicht abbaubaren algenbürtigen Kohlenstoffverbindungen aus dem Fluss in das Ästuar führt im Sommer zu heterotrophen Bedingungen im Elbe-Ästuar und als Folge zu Sauerstoffdefiziten.

Mit dem großskaligen eindimensionalen Modellansatz wird zudem für einen 13-jährigen Zeitraum (1998-2010) die Wassertemperatur, das Phytoplankton und der Sauerstoff für den Flusslauf und das Ästuar simuliert und validiert. Darüber hinaus werden neue Entwicklungen vorgestellt, wie das Modell QSim mit mehrdimensionalen hydrodynamischen Modellen offline gekoppelt und betrieben werden kann. Für ein Testgebiet wird die horizontale Verteilung der Wassertemperatur in einem durch Nebenrinnen charakterisierten Abschnitt des Ästuars simuliert und mit Beobachtungswerten verglichen.

Schlagwörter

Gewässergütemodell, Elbe-Ästuar, Wassertemperatur, Sauerstoff, Phytoplankton

Contents

1	Introduction	204
2	The model QSim	206
2.1	Concept of coupling QSim with hydrodynamic drivers.....	206
2.2	Description of QSim modules.....	207
3	QSim application for the Elbe and its estuary	211
3.1	Model area	211
3.2	Boundary conditions	212
3.3	Model calibration	213
4	Results	215
4.1	Water levels in the estuary	215
4.2	Longitudinal profiles of water quality parameters	216
4.3	Validation of the long term simulation of water quality parameters	221
4.4	Simulation of water temperature distribution in the Elbe Estuary with 2d QSim.....	225
5	Discussion	225
6	Conclusions and outlook	228
7	Acknowledgements.....	229
8	References	229

1 Introduction

Water quality conditions and management in estuaries have received increasing attention in recent years. One significant ecological issue in estuaries and adjacent coastal waters is

the appearance of low oxygen conditions (hypoxia) (RABALAIS et al. 2009, HOWARTH et al. 2011, ZHU et al. 2011).

It has been shown for many river systems that excessive nutrient loading in the catchment can foster phytoplankton blooms and eutrophication in the middle and lower part of rivers (SALMASO and BRAIONI 2008, PUSCH et al. 2009). The high organic matter load caused by phytoplankton leads to heterotrophic conditions in the estuaries of eutrophic rivers, mainly indicated by oxygen deficits (PAERL and PINCKNEY 1998, GARNIER et al. 2001). In well-mixed estuaries, the longitudinal location of low oxygen zones seems to be specific for each estuary. While in less eutrophied estuaries the oxygen minimum often occurs in the maximum turbidity zone, the oxygen minimum in more heavily loaded estuaries can be observed in the freshwater section (GARNIER et al. 2001). In addition to the amount of organic matter loading and the amount of freshwater (river discharge) entering the estuary, the bathymetry is an important factor influencing the oxygen concentration in the estuary.

In the freshwater zone of the Elbe Estuary, low oxygen conditions in summer regularly occurred during the last four decades. The phenomenon of hypoxia in the Elbe Estuary has been described by CASPERS (1984), ARGE ELBE (1984), FLÜGGE (1985) and more recently by BERGEMANN et al. (1996) and YASSERI (1999).

While most of the biogeochemical processes of oxygen depletion in estuaries are qualitatively well-known, a temporally and spatially detailed quantitative analysis is needed to fulfil requirements concerning management strategies, e.g. eutrophication control by nutrient reduction. Numerical modelling of surface water quality can be a useful tool to support these analyses and has been used extensively as a scientific and management tool to analyse and quantify oxygen deficits in estuaries (BILLEN et al. 2001, ZHENG et al. 2004).

This paper presents an approach of numerical modelling of water quality, particularly water temperature, algal as well as zooplankton development and oxygen conditions, in the German part of the Elbe and its estuary. To simulate water quality components, the physical transport and the biogeochemical processes have to be linked. Therefore, a hydrodynamic model is coupled with a water quality model simulating the biogeochemical processes. This general model coupling approach was realized in the Chesapeake Bay Model Package (CBMP) by CERCO and COLE (1993) and is nowadays realized in many "software families". Recently, a coupled hydrodynamic and biogeochemical model for the Schelde Estuary is applied by ARNDT et al. (2011) and GYPENS et al. (2013). Other developments are concepts of dynamic coupling of hydrodynamic models to biogeochemical moduls, such as Framework of Aquatic Biogeochemical Models (FABM) (BRUCE et al. 2013).

The model coupling approach can be applied for one or more dimensions to fulfil different resolutions in space, depending on the investigation objectives. In 1d model approaches, the systems are strongly simplified by considering a fully mixed water body and by neglecting lateral as well as vertical resolution. Nevertheless, these approaches are successfully used for large scales (where dominant longitudinal gradients exist) like catchments or large river sections, especially in the context of global change studies (BILLEN et al. 2001, DUCHARNE et al. 2007, QUIEL et al. 2011). In contrast, more-dimensional approaches are useful concerning the research on a smaller scale like harbour basins, distinct bays and also whole estuaries in which drying and flooding plays a major role.

2 The model QSim

The water quality model QSim simulates physical, chemical and biological processes in rivers (KIRCHESCH and SCHÖL 1999; SCHÖL et al. 2002, MATZINGER et al. 2013). QSim was established in the 1980s and has been expanded and improved since then (SCHÖL et al. 2006 a/b, BECKER et al. 2010, QUIEL et al. 2011).

QSim is a deterministic model with a modular structure, i.e. processes concerning the heat budget, nutrient as well as oxygen budget and plankton development are described as separate modules in the form of differential and algebraic equations without any stochastic effect.

2.1 Concept of coupling QSim with hydrodynamic drivers

A hydrodynamic model is needed for water quality simulation with QSim. Depending on the dimension of the hydrodynamic model, a 1d, 2d or 3d QSim simulation of water quality can be achieved. The 1d approach of QSim is coupled off-line with HYDRAX (OPPERMANN 1989). QSim and HYDRAX are integrated by the graphical user interface GERRIS (BFG 2013). The 2-dimensional approach of QSim has been recently coupled off-line with casu (WYRWA 2003) (Fig. 1). In this approach, the existing QSim code is embedded as FORTRAN-subroutines by implementation of shell-routines wrapping.

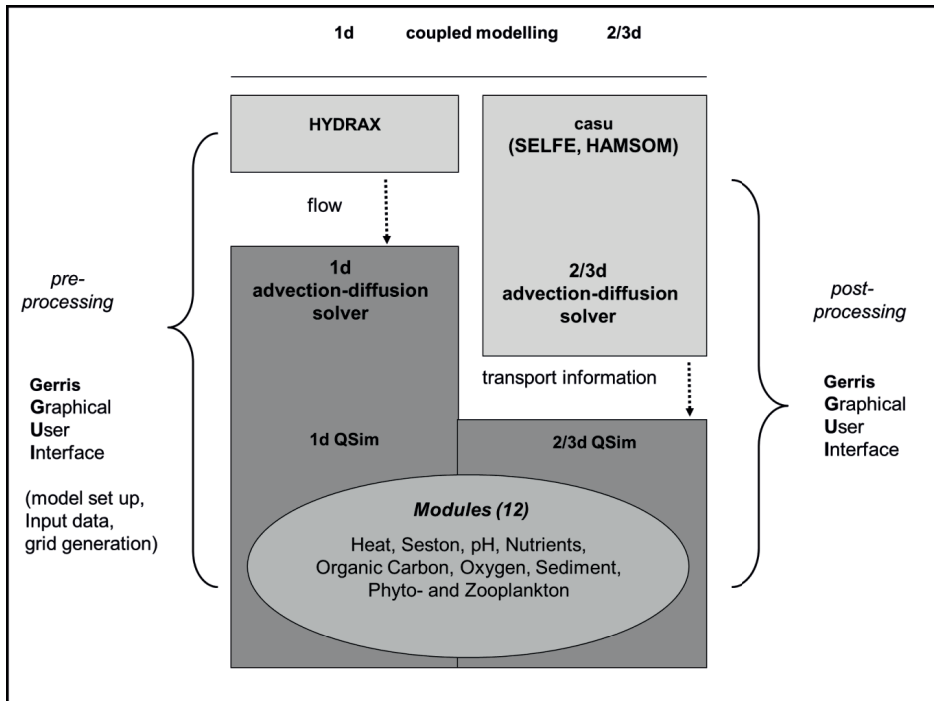


Figure 1: Concept of coupling between the water quality model (QSim) and hydrodynamic models (HYDRAX or casu).

1d QSim approach with HYDRAX

HYDRAX is a 1d hydrodynamic model to simulate unsteady flow in a network of water bodies (OPPERMANN 1989, 2010). In HYDRAX, the Saint Venant equations are solved numerically with the implicate difference scheme of Preismann (CUNGE et al. 1980). The non-linear system of equations is solved iteratively with two different Double Sweep methods for tree-based and network-based graphs (CUNGE et al. 1980, FRJASINOV 1970). The flow can be calculated either in a stationary or in a dynamic non-stationary way. HYDRAX calculates the hydraulic conditions (river discharge, water level, mean water depth, and flow velocity) along the river stretch using cross-sectional profiles, bed roughness and slope of the river stretch. At the upper boundary and the inflowing tributaries, measured river discharge is prescribed. At the lower boundary HYDRAX is forced by measured water levels. Data on the hydraulic conditions along the investigated water body are provided to QSim using the common grid structure.

Water quality input data are needed for the tributaries, for the upper and - in case of modelling an estuary with tidal changes of the flow direction – for the lower model boundary in order to indicate the starting conditions for model calculations. Generally, the biogeochemical processes in QSim are computed on an hourly basis. Due to stability reasons, sub-time steps are used to calculate the advection and diffusion of the 70 biological variables. For the case study Elbe, the second-order QUICKEST transport algorithm, which includes a limiter function, is used (LEONARD 1961).

2d QSim approach with casu

The 3d flow solver casu (WYRWA 2003), which is based on the numerical proposals of CASULLI and CHENG (1992), is used as a hydrodynamic driver. It solves the 3d shallow water equations. When discretised with only one depth layer, the computation is reduced to a 2d depth-averaged model. At downstream/seaward boundaries water levels are set, which is appropriate also for flow reversal in tidal motion. At upstream/landward boundaries model data from the 1d approach are used. Internally casu distributes both hydrodynamic conditions along the boundary faces. The water level is set constant along the downstream boundary line. The flow velocities at the boundaries are distributed assuming that each vertical would be a straight rough channel and all verticals have the same water level slope. Casu computes transient solutions. Stationary flow fields are obtained when the flow converges gradually to stationary boundary conditions. The 3d hydrodynamic driver casu in contrast to the 1d hydrodynamic model HYDRAX already includes an advection-diffusion (transport) solver which is needed for hydrodynamically active concentrations (salt, suspended sediment) and turbulence quantities. Casu uses ELM for advection and finite differences for diffusion (WYRWA 2003). The offline stored transport-matrices can be used directly by QSim by multiplication with the concentration fields (discretised as vectors).

2.2 Description of QSim modules

The model QSim comprises twelve modules that can be grouped into a heat module, which calculates the water temperature, seven biogeochemical modules for process description of the seston budget, pH-value, nutrients dynamics of nitrogen (N), phospho-

rous (P) and silicium (Si), organic carbon and oxygen content, three biological modules for phyto- and zooplankton and benthic filter feeders (not applied for the Elbe) and a sediment module which calculates early diagenesis of sediment dynamics including oxygen, carbon and nutrient fluxes. For all modules we hereby provide brief descriptions and references. Input variables and parametrisation of processes are given in Tab. 2 and 3.

Heat module

The basis for calculating the heat budget of a water body is the simplified heat balance equation. The water temperature is influenced by radiation (q_S), evaporation (q_V), convection (q_K), the temperature of the riverbed (q_{US}), the sediment-water heat exchange (q_U) and direct discharges (q_E), i.e. tributaries and thermal power stations, into the river. Input variables are measured data of global radiation, air temperature, relative humidity, cloudiness, and wind velocity (Tab. 2) at distinct sites of the model area. Further information of components and their parameterisation are given in IKSR (2013).

The heat balance equation can be written as:

$$\frac{\partial T_W}{\partial t} = \frac{q_S - q_V - q_K + q_{US} - q_U + q_E}{c_W * H * \rho_W} \quad (1)$$

T_W - water temperature [°C]

t - time [h]

q_S - heat flux from radiation [kJ*h⁻¹*m⁻²]

q_V - heat flux from evaporation [kJ*h⁻¹*m⁻²]

q_K - heat flux from convection [kJ*h⁻¹*m⁻²]

q_{US} - heat flux from radiation into the sediment [kJ*h⁻¹*m⁻²]

q_U - sediment - water heat exchange [kJ*h⁻¹*m⁻²]

q_E - heat flux from direct discharge [kJ*h⁻¹*m⁻²]

c_W - special heat capacity of water = 4.1868 10³ J*kg⁻¹*K⁻¹

H - average water depth of the cross section [m]

ρ_W - density of the water = 1,000 kg*m⁻³

However, this equation of the heat balance cannot be solved explicitly, as the different components are not independent of each other. Therefore, the equation is solved by iteration, taking into account that short time steps for iteration should be used in cases of low water depth in order to avoid large differences in water temperature during the iteration loops.

Biogeochemical modules

Nutrients (N, P, Si)

QSim calculates the important processes of the cycling of nutrients (KIRCHESCH and SCHÖL 1999). The nitrogen components are total nitrogen, ammonium, nitrite and nitrate. Main processes are assimilation by phytoplankton, ammonification by decay of organic matter, nitrification and denitrification. The growth of suspended nitrifiers (*Nitrosomonas* and *Nitrobacter*) is depending on water temperature, oxygen concentration and substrate concentration (ammonium or nitrite). The nitrification/denitrification process and the N-fluxes from/to the sediment are implemented in the sediment module. The balance of the particulate fraction of total phosphorus and the dissolved fraction of

ortho-phosphate is simulated. While ortho-phosphate is lost due to assimilation by algae, it is produced by respiration of algae, rotifers and benthic filter feeders (mussels) as well as by the decay of detritus. Faeces released by rotifers and benthic filter feeders are sources of ortho-phosphate after bacterial degradation. Dissolved silica is modelled, because it is a structural element of the cell wall of diatoms and can limit their growth. Besides the silica uptake by diatoms, a release of silica from the sediment during decay of diatoms is considered in the model.

Organic carbon

The hydrolysis of the biodegradable organic matter fractions to monomeric substances is calculated following the conceptual model of organic matter degradation by BILLEN (1991), who gave a general view of bacterial growth in aquatic systems. The organic matter is divided into five fractions, where the particulate refractory organic matter is a permanent sink and not linked to degradation processes by bacteria. The four other fractions are biodegradable, characterized by different hydrolysis rates. The biomass of each biological group that enters the organic matter fractions by mortality, excretion or in form of faeces is added equally to each of the five fractions. The substrate uptake rate of bacteria only depends on the available concentration of monomeric substances:

$$up_{Bac} = up_{Bac,max} * \frac{C_M}{C_M + K_{S,C_M}} * f_{Bac}(T) \quad (2)$$

- $up_{Bac,max}$ - maximal uptake rate of bacteria [d⁻¹]
- C_M - concentration of monomeric substances [mgC*l⁻¹]
- K_{S,C_M} - half saturation constant of bacteria for monomeric substances [mgC*l⁻¹]
- $f_{Bac}(T)$ - temperature dependence ratio [-]

In the QSim modelling approach, bacterial biomass is linked to total biodegradable carbon and to the degradability of the substrate. Both variables are derived from the ratio between carbon-based BOD₅ and chemical oxygen demand (COD). This approach enables to calculate the bacterial biomass from routine measurements, although the bacterial biomass itself was not measured (BERGFELD 2002).

Biological modules

Phytoplankton

In QSim, three major taxonomic phytoplankton groups with different physiological characteristics can be distinguished (Tab. 2). The algal biomass balance is:

$$\frac{dA}{dt} = (\mu - k_{resp} - k_{mort}) * A - A_{graz} - A_{sed} \quad (3)$$

- A - algal biomass [mg*l⁻¹]
- μ - actual growth rate [d⁻¹]
- k_{resp} - respiration rate [d⁻¹]
- k_{mort} - mortality rate [d⁻¹]
- A_{graz} - grazing losses [mg*l⁻¹*h⁻¹]
- A_{sed} - sedimentation losses [mg*l⁻¹*h⁻¹]
- t - time [h]

The effective limitation of phytoplankton growth by the three parameters temperature, light and nutrients is calculated by multiplying the production rate with the limitation factors of these parameters (SCHÖL et al. 2002; SCHÖL et al. 2006a).

$$\mu = P_{mean} * (Chla : C) * f_T * f_N * f_L \quad (4)$$

- P_{mean} - mean production rate in the vertical profile [mgC* mgChla⁻¹*h⁻¹]
- $Chla : C$ - chlorophyll-a/carbon ratio [mgChla*mgC⁻¹]
- f_T - effect of temperature on growth rate [-]
- f_N - effect of nutrients on growth rate [-]
- f_L - effect of light (photo-inhibition) on growth rate [-]

Nutrient limitation is defined by the most limiting nutrient.

$$f_N = \min \left(\left(N / (k_N + N) \right); \left(P / (k_P + P) \right); \left(Si / (k_{Si} + Si) \right) \right) \quad (5)$$

- $k_{N, P, Si}$ - half saturation constant of nutrient x [mg*l⁻¹]
- N - nitrogen concentration [mg*l⁻¹]
- P - phosphorus concentration [mg*l⁻¹]
- Si - silicate concentration [mg*l⁻¹]

Light limitation is calculated taking into account the quantum yield of phytoplankton during its transport through the vertical light gradient as well as the (light-dependent) chla/carbon ratio (OLLINGER 1999).

Zooplankton

Zooplankton is represented by rotifers as described in SCHÖL et al. (2002). In the Elbe, rotifers are the dominant group (HOLST 2006). Crustaceans become an important group in the estuary of the Elbe, but no separate modelling approach for this group is implemented in QSim.

$$\frac{dROT}{dt} = (\mu_{ROT} - resp_{b,ROT} - mort_{ROT}) * ROT \quad (6)$$

- ROT - biomass of rotifers [mgC*l⁻¹]
- μ_{ROT} - growth rate [d⁻¹]
- $resp_{b,ROT}$ - basic respiration rate [d⁻¹]
- $mort_{ROT}$ - mortality rate [d⁻¹]

Sediment module

The sediment module is designed after DI TORO (2001) as a two layer approach with a separate implementation for oxic and anoxic processes, respectively. Flux calculations take place at each time step to realize a dynamic pelagic-benthic coupling. Further details are described in BFG, 2013).

3 QSim application for the Elbe and its estuary

The description of the model area, boundary conditions, model calibration and parametrisation refer to the 1d QSim approach with HYDRAX. Model-specific options concerning the 2d approach (QSim coupled with casu) are mentioned.

3.1 Model area

The Elbe has a length of 1,094 km from its spring in the Giant Mountains (Czech Republic) to the North Sea (Germany). The main German tributaries are Schwarze Elster, Mulde, Saale and Havel.

The model area of the 1d approach starts about 367 km below the source of the Elbe at the border between the Czech Republic and Germany (Elbe-km 0) and reaches until the North Sea at Cuxhaven (Elbe-km 727). It comprises the stretch of the Elbe River up to the tidal weir of Geesthacht (km 0 to km 585) and the Elbe Estuary (km 585 to km 727) (Fig. 2). The estuary can be divided into a freshwater region (< 0.5 PSU), an oligohaline zone (0.5-5 PSU) and a mesohaline zone (5-18 PSU). These salinity limits are according to the “Venice System”. The zones have been determined based on a longitudinal salinity profile measured by the River Basin Community Elbe (FGG Elbe: <http://www.fgg-elbe.de/fgg-elbe.html>) on the 24/08/2006 at ebb tide. The mean discharge during the period 24/07/2006 to 24/08/2006 has been 413 m³*s⁻¹ at the station Neu Darchau (km 536).

The tributaries are considered as lateral boundaries. The river stretch is divided into 1622 segments. Generally, the spatial resolution of the river and the estuary is 500 m. The 1d approach is extended by the implementation of groyne fields influencing the main river by lateral transfers (SCHÖL et al. 2006a). The complete river stretch is modelled to get a consistent input data set for the water quality simulation of the estuary.

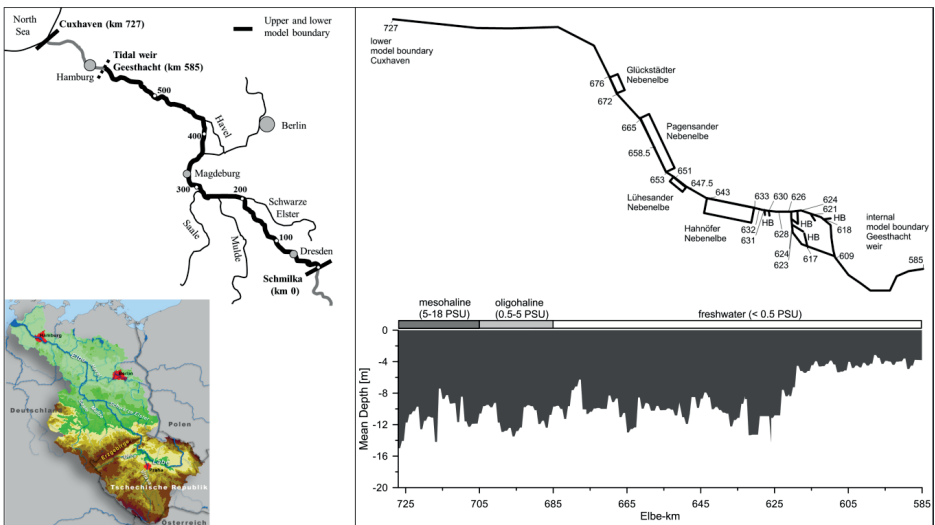


Figure 2: Entire model area (left) and 1d model structure of the Elbe Estuary with longitudinal profile of modelled mean water depth [m] (right) and salinity zonation. HB – Harbour Basin.

The 2d model approach covers only the Elbe Estuary. The irregular triangle mesh contains 42,442 nodes and 76,357 elements with a mean edge-length of 90 m ranging from 4.6 m to 440 m and a mean element size of 5,300 m² ranging from 18 m² to 120,000 m². For the 2d QSim approach, the biological and physical-chemical boundary conditions at the upstream inflow at Geesthacht (km 585) are taken from 1d model results. In Tab. 1, the hydrological properties of the 1d as well as the 2d approach are listed.

Table 1: Water volume [km³], water surface [km²] and mean depth [m] of the Elbe Estuary.

Model Elbe Estuary	Volume [km ³]	Water surface [km ²]	Mean Depth [m]
1d	2.3	245.9	8.2
2d	2.4	305	7.7

3.2 Boundary conditions

The 1d QSim application of the Elbe and its estuary uses a considerably set of input variables at all boundaries and for the atmospheric forcing (Tab. 2). For 2d QSim temperature simulations, the same meteorological forcing as in the 1d approach is applied, using the records from weather stations in Hamburg and Cuxhaven. Water temperatures at the upper boundary of the 2d approach at the weir of Geesthacht are based on the 1d model results.

Table 2: Input data needed for water quality modelling with QSim.

Morphological/ hydrological: Bathymetry (cross sections), discharge, water level
Meteorological: Global radiation, air temperature, cloud cover, relative humidity, wind velocity
Biological: Biological oxygen demand (carbon-derived, C-BOD and nitrification-derived, N-BOD), biomass of planktonic algae (chlorophyll a) and proportion of diatoms, green algae and cyanobacteria, zooplankton biomass, biomass of nitrifiers
Physical-chemical: Water temperature, oxygen, chemical oxygen demand, total nitrogen, nitrate, nitrite, ammonium, silicate, alkalinity, seston, total phosphor, ortho - phosphate, calcium, conductivity

Hydrology and water level

The upper model boundary at km 0 is forced with daily discharge data. For the four main tributaries (Schwarze Elster, Mulde, Saale, Havel) and six other large tributaries, daily discharge data are used, while for eight smaller tributaries only yearly mean discharge is considered. Depending on availability, daily or monthly data are applied for the sewage plants. The lower model boundary is forced with the water level of the gauging station Cuxhaven-Steubenhöft.

Meteorology

The following parameters have been provided as daily data by the German Weather Service for the years 1998-2010: daily sum of the global solar radiation (J*cm⁻²), minimum and maximum air temperature (°C), mean relative humidity (%), mean wind velocity (m*s⁻¹) and mean cloud cover. Along the river stretch the data of four stations (Dresden, Wittenberg, Magdeburg, Seehausen) and for the estuary of two stations (Hamburg and

Cuxhaven) are used. The solar radiation is not recorded at the station Magdeburg and Cuxhaven, and is therefore replaced by data of the nearby stations of Braunschweig respectively Hamburg.

Water quality parameters and phytoplankton biomass

Water quality parameters are provided by the River Basin Community Elbe (FGG Elbe) and by the Observational Network of Water Quality of Hamburg (Institute of Hygiene and Environment). The water quality data at Schmilka (km 3.9) and Cuxhaven (km 727) are used to force the model at the open boundaries. The data of the following stations are used for the main tributaries: Gorsdorf (Schwarze Elster), Dessau (Mulde), Rosenberg (Saale) and Toppel (Havel).

The main sewage plants situated in the river stretch of the Elbe (Dresden-Kaditz and Magdeburg-Gerwisch) as well as in the Elbe Estuary (Hamburg-Dradenau) are also implemented in the model.

3.3 Model calibration

Water level

The water level is calculated by the 1d hydrodynamic model HYDRAX. To characterise the flow, different zones can be differentiated (retention area, floodplain, main channel). For every zone, a different Manning roughness coefficient can be set.

For the Elbe a constant Manning coefficient is used for each zone (main channel $40 \text{ m}^{1/3}\text{s}^{-1}$, floodplain $12 \text{ m}^{1/3}\text{s}^{-1}$, retention area $0 \text{ m}^{1/3}\text{s}^{-1}$). For the Elbe Estuary, the roughness of the main channel is represented by a function of the roughness coefficient depending on the water level as shown in Fig. 3. For the floodplains of the estuary the same approach is applied using a factor of 0.3. The value for the retention area of the estuary is set to the same value like in the river stretch of the Elbe.

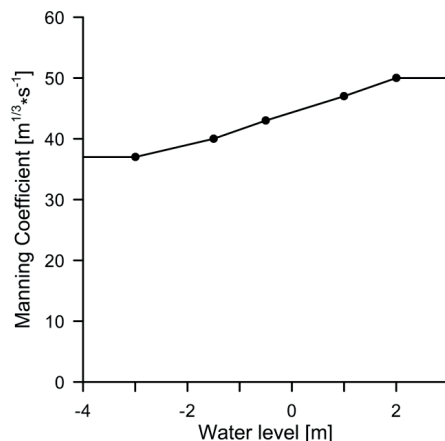


Figure 3: Manning roughness coefficient [$\text{m}^{1/3}\text{s}^{-1}$] used for the main channel of the Elbe Estuary.

Biological Parameters

The standard set of parameters which is either based on literature or on own experimental results was adjusted for the Elbe Estuary (Tab. 3). The light saturation for diatoms and green algae was increased, the maximum growth rate decreased. The adaptations were performed to reflect the specific species composition of the Elbe. The coefficient of absorption for yellow substances (humics) at 440 nm was increased by the factor 10 to parameterise the effect of high seston content of the Elbe Estuary.

Zooplankton abundances are not recorded in the regular monitoring programme of the Elbe. Therefore, abundances at the upper (km 0) and the lower (km 727) boundaries are estimated with the value of 25 Ind*1⁻¹. This low abundance is sufficient as an inoculum to enable the development of the zooplankton in dependency of the food supply by phytoplankton.

Table 3: List of parameters for green algae, diatoms, cyanobacteria, rotifers, nitrifiers and others in Qsim.

Parameter	Unit	Value
Green Algae / Diatoms / Cyanobacteria		
Chlorophyll/Biomass ratio	$\mu\text{gChla}*\text{mgBio}^{-1}$	21.5/21.5/21.5
Maximum growth rate	d^{-1}	1.6/ 1.3/ 1
Light saturation of the photosynthesis	$\mu\text{E}*m^{-2}*s^{-1}$	176/ 78/ 34
Half saturation constant Nitrogen (N)	$\text{mg}*\text{l}^{-1}$	0.048/ 0.018/ 0.02
Half saturation constant Phosphorus (P)	$\text{mg}*\text{l}^{-1}$	0.022/ 0.02/ 0.02
Half saturation constant Silicium (Si)	$\text{mg}*\text{l}^{-1}$	-/ 0.08/ -
Basic respiration	d^{-1}	0.085
Proportion of growth dependend respiration rate	-	0.2
C-BOD ₅ of phytoplankton		0.004/0.021/0.004
COD of phytoplankton		0.073/0.105/0.073
Maximum cell quota N	$\text{mg}*\text{mgBio}^{-1}$	0.049/ 0.1/ 0.085
Maximum cell quota P	$\text{mg}*\text{mgBio}^{-1}$	0.012/ 0.009/ 0.007
Maximum cell quota Si	$\text{mg}*\text{mgBio}^{-1}$	-/ 0.18/ -
Minimum cell quota N	$\text{mg}*\text{mgBio}^{-1}$	0.008/ 0.017/ 0.014
Minimum cell quota P	$\text{mg}*\text{mgBio}^{-1}$	0.0016/ 0.0011/ 0.0009
Minimum cell quota Si	$\text{mg}*\text{mgBio}^{-1}$	-/ 0.18/ -
Maximum uptake rate N	d^{-1}	0.09/ 0.31/ 0.31
Maximum uptake rate P	d^{-1}	0.69/ 0.62/ 0.62
Maximum uptake rate Si	d^{-1}	-/ 2.5/ -
Minimal O ₂ production	$\text{mg O}_2*\text{mgBio}^{-1}$	1.3
Maximal O ₂ production	$\text{mg O}_2*\text{mgBio}^{-1}$	1.8
Intensity of sedimentation	between 0 and 1	0.5/0.5/0
Temperature optimum	°C	33.5/20/26
Lethal temperature	°C	47/31/35
Rotifers		
Maximum ingestion rate	$\mu\text{gC}*\mu\text{gC}^{-2/3}*\text{d}^{-1}$	2.9
Half-saturation constant for C ingestion	$\text{mg}*\text{l}^{-1}$	0.43
Biomass (dry mass)	μg	0.3
Basic respiration	d^{-1}	0.12

Parameter	Unit	Value
Filterability of diatoms	0-1	0.6
Filterability of green algae	0-1	0.8
Filterability of cyanobacteria	0-1	0.1
Nitrifier		
Maximum growth rate Nitrosomonas	d ⁻¹	1.08
Half saturation constant Nitrosomonas	mg NH ₄ -N*l ⁻¹	0.48
Mortality rate Nitrosomonas	d ⁻¹	0.1
Maximum growth rate Nitrobacter	d ⁻¹	1.1
Half saturation constant Nitrobacter	mg NO ₂ -N*l ⁻¹	1.3
Mortality rate Nitrobacter	d ⁻¹	0.1
Other		
Maximum NH ₄ oxidation rate in sediments	m*d ⁻¹	0.25
Maximum denitrification rate in sediments	m*d ⁻¹	0.32
Hydrolysis rate for easily degradable particulate organic C-compounds	d ⁻¹	0.12
Hydrolysis rate for easily degradable dissolved organic C-compounds	d ⁻¹	18
Half saturation constant for hydrolysis of easily degradable dissolved organic C-compounds	mgC*l ⁻¹	0.25
Half saturation constant for hydrolysis of poorly degradable dissolved organic C-compounds	mgC*l ⁻¹	2.5
Half saturation constant for degradation of monomer C-compounds	mgC*l ⁻¹	0.1
Maximum uptake rate of monomer C-compounds of bacteria	d ⁻¹	24.7
Yield coefficient for bacteria biomass	-	0.25
Basic respiration heterotrophic bacteria	d ⁻¹	0.03
Absorption coefficient for yellow substances/humics at 440 nm	-	7.5

4 Results

4.1 Water levels in the estuary

For the station St. Pauli (km 623) measured and modelled water levels are compared for the 1d model HYDRAX and the 2d model casu (Fig. 4a and b). The hydrodynamic model HYDRAX simulates the point in time of high tide and low tide accurately. The amplitudes are also reproduced well. However, the values of the low tide are often underestimated. Based on hourly measured and simulated data for the period 25/09/2006 to 09/10/2006 the mean difference referring to the absolute values between measurements and simulations is 0.11 m.

Based on 15 min values simulated by the 2d approach with casu the mean difference for the period 03/07/2010 to 17/07/2010 is 0.10 m.

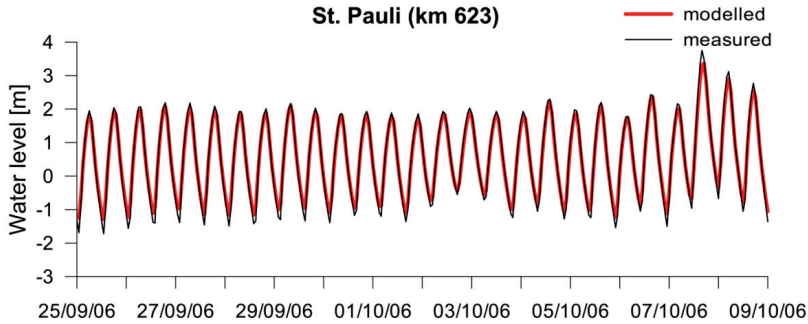


Figure 4a: Measured (black line) and modelled (red line) water levels [m] of the 1d model HY-DRAX at St. Pauli (km 623) for the period 25/09/2006 to 09/10/2006 (measured data: Hamburg Port Authority).

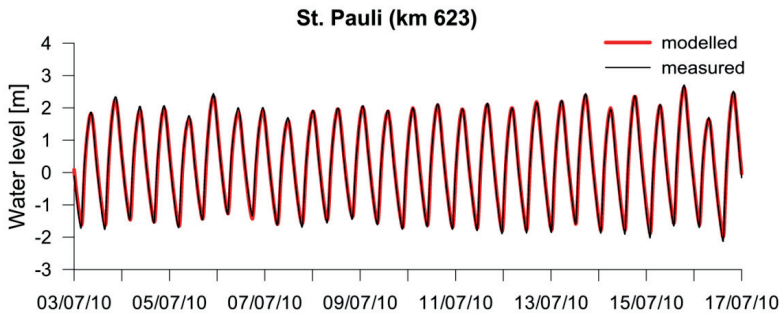


Figure 4b: Measured (black line) and modelled (red line) water levels [m] of the 2d model casu at St. Pauli (km 623) for the period 03/07/2010 to 17/07/2010 (measured data: Hamburg Port Authority).

4.2 Longitudinal profiles of water quality parameters

The 1d QSim simulations of the year 2006 are compared with measured data. Therefore, a seasonal mean from 01/05/2006 to 31/10/2006 as a representative value for the vegetation period is used. This period has beneficial conditions for algal growth due to sufficient global radiation, high water temperatures and low discharge conditions leading to water retention times in the river (km 0 to km 586) of more than 5 days.

For the considered period the position of the salinity threshold of 0.5 PSU was located at Brokdorf km 685 meaning that the freshwater region of the estuary comprised about 100 km until the tidal weir of Geesthacht (km 585) (Fig. 2).

Phytoplankton

The inoculum of algal biomass at the model boundary (km 0) is high with a mean value of $54 \mu\text{g chla} \cdot \text{l}^{-1}$. The longitudinal development of the phytoplankton is shown by the seasonal mean chla values and their standard deviations (Fig. 5). Both the modelled and the measured mean chla values increase along the river. The modelled values end up with a maximal mean of $143 \mu\text{g} \cdot \text{l}^{-1}$ at km 574 just some kilometres upstream the weir of Geesthacht (km 585), while the measured values reached $167 \mu\text{g} \cdot \text{l}^{-1}$ at km 598, just some

kilometres below the weir. Along the estuary, the algal biomass declines sharply. At km 660 near the seaward limit of the freshwater region a low mean value of $6 (\pm 9) \mu\text{g chl}a \cdot \text{l}^{-1}$ is calculated by the model. Measurements at that site have a seasonal mean of $12 (\pm 5) \mu\text{g chl}a \cdot \text{l}^{-1}$.

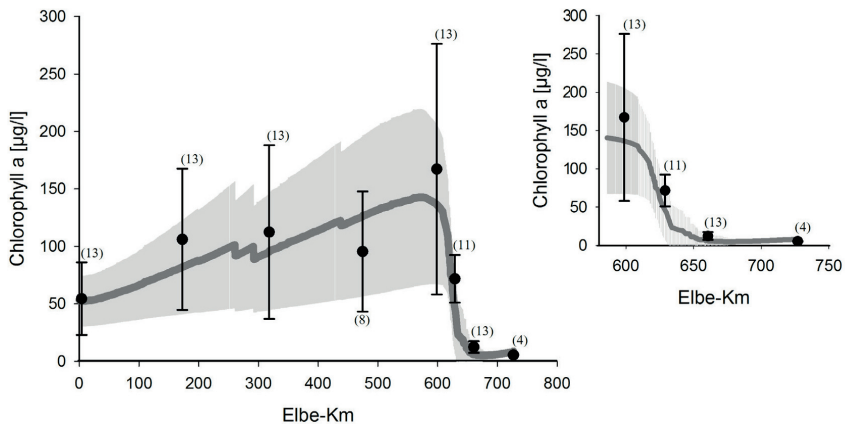


Figure 5: Longitudinal profile of measured (black dots) and modelled (dark grey line) seasonal means of chlorophyll a [$\mu\text{g} \cdot \text{l}^{-1}$] from Schmilka (km 0) to Cuxhaven (km 727) for May to October 2006. Number of measurements is given in brackets. Standard deviations of measurements reflected by bars and of modelled data ($n = 184$) by the light grey area.

Beside the coincident increase and decrease of the modelled and measured seasonal chla means, it is noteworthy that the standard deviations (σ) of model data and measurements have the same magnitude and longitudinal pattern. In the river, a wide range of chla concentrations are measured giving a high σ . This is mainly caused by changing discharge conditions, which cause different development times for algae in the river. This dependency is already indicated by the boundary values. The simulation reflects this pattern well. A correlation of the chla content in relation to the discharge conditions at km 586 shows a weak negative correlation with a $r^2 = 0.21$. In the estuary the seasonal variability of chla is only notable for the upper section, already at km 629 σ is lowered to $20 \mu\text{g chl}a \cdot \text{l}^{-1}$ with the measured mean of $71 \mu\text{g chl}a \cdot \text{l}^{-1}$. Concerning the modelling results the range of σ is $38 \mu\text{g chl}a \cdot \text{l}^{-1}$ related to a mean value of $45 \mu\text{g chl}a \cdot \text{l}^{-1}$. The σ -value is diminished even more at km 660 (values given above). At the estuarine sites the seasonal variability of the chla concentration becomes less influenced by river discharge, but, as shown by analysing the model results, increasingly influenced by zooplankton grazing.

Zooplankton

For the season in 2006 the simulations show a mean increase of zooplankton (represented by the rotifer *Brachionus sp.* in the QSim model approach) along the river stretch from estimated $25 \text{ Ind} \cdot \text{l}^{-1}$ at the upper boundary at km 0 to $160 \text{ Ind} \cdot \text{l}^{-1}$ at km 470 and $318 \text{ Ind} \cdot \text{l}^{-1}$ at km 586 at the entrance to the estuary (data not shown). In the estuary, the development of zooplankton is strongly enhanced due to both optimal food supply and long residence times. In the area of the harbour the model results show a seasonal mean

of 1,482 Ind* l^{-1} and a maximum abundance of up to 4,256 Ind* l^{-1} (km 629). Further downstream the mean abundances decrease rapidly below 500 Ind* l^{-1} at km 660.

There are only very few counted zooplankton data available, but in 2006 biweekly sampling at Cumlosen (km 470) by the Environmental Agency of Brandenburg and at Seemannshöft (km 629) by the Institute of Hygiene and Environment, Hamburg took place. Between 10 and 20 l water volume was filtered through a net of 55 μ m meshes. The fixed samples were counted under an inverse microscope. Seasonal means of the year 2006 of the rotifer and crustacean zooplankton were 555 and 81 Ind* l^{-1} at km 470 (n = 13) as well as 822 and 221 Ind* l^{-1} at km 629 (n = 12).

Based on the modelled zooplankton abundances the grazing rates along the Elbe and in the estuary are calculated. Our 1d modelling approach identifies grazing as the dominant loss process for phytoplankton in the Elbe Estuary. Seasonal mean (May – October) grazing rates in the river at km 470 reach only 0.02 per day, but rise up to 0.5 per day with a maximum of 2.0 per day in the estuary at km 629.

BOD

Closely related to the algal development, the modelled seasonal mean C-BOD₅ increases along the river from 5.3 mg O₂* l^{-1} at the start (model boundary) to a maximum of 7.0 mg O₂* l^{-1} at km 577. In the estuary the mean values decrease from 5.5 mg O₂* l^{-1} at km 629 down to values below 3 mg O₂* l^{-1} at km 653 (Fig. 6). Because the C-BOD₅ is not part of the Elbe monitoring programme, the measured BOD₇ is applied for comparison. Because the incubation period differs by two days and the BOD includes the oxygen consumption by nitrification, the modelled C-BOD₅ value is multiplied the factor 1.5 to get the same range of values for both parameters. Due to methodologically caused high variation of the parameter and a low number of samples, the measured mean BOD₇ values do not show a clear trend in the river (range between 4.7 to 7.7 mg O₂* l^{-1}), but at the estuarine stations a clear decrease from 5.6 mg O₂* l^{-1} at km 629 down to values not higher than 2 mg O₂* l^{-1} is obvious.

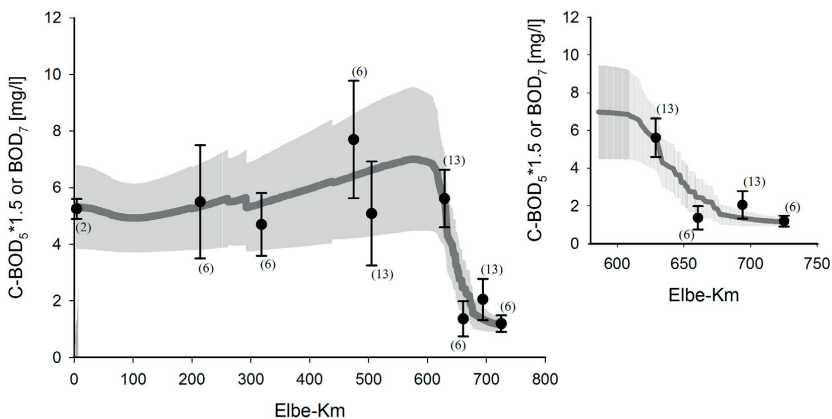


Figure 6: Longitudinal profile of seasonal means of measured BOD₅ [mg* l^{-1}] (black dots) and modelled C-BOD₇ [mg* l^{-1}] (dark grey line) from Schmilka (km 0) to Cuxhaven (km 727) for May to October 2006. Number of measurements is given in brackets. Standard deviations of measurements reflected by bars and of modelled data (n = 184) by the light grey area.

Oxygen

The measured seasonal mean oxygen content is derived from continuous measurements by probes at the given monitoring sites (FGG Elbe: <http://www.fgg-elbe.de/fgg-elbe.html>). Along the river the measured mean values increase from 9.6 mg O₂*l⁻¹ at km 4 up to 12.6 mg O₂*l⁻¹ at km 474, while the maximum modelled value is reached at km 566 with a slightly lower maximum of 11.1 mg O₂*l⁻¹ (Fig. 7).

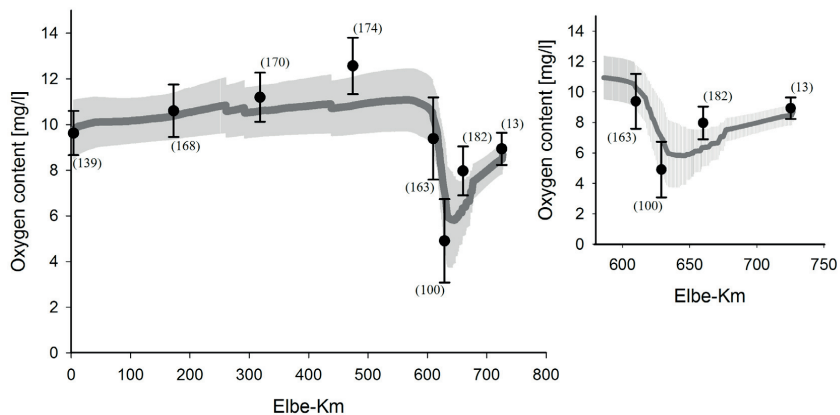


Figure 7: Longitudinal profile of measured (black dots) and modelled (dark grey line) oxygen content [mg*l⁻¹] from Schmilka (km 0) to Cuxhaven (km 727) for May to October 2006. Number of measurements is given in brackets. Standard deviations of measurements reflected by bars and of modelled data (n=184) by the light grey area.

Entering the estuary the oxygen content still remains high (measured: 9.4 mg O₂*l⁻¹; modelled: 10.4 mg O₂*l⁻¹) at km 609, the upper end of the Hamburg harbour. Further downstream a strong decrease of oxygen is measured and modelled, reaching an observed mean minimum at km 629 with 4.9 (± 1.83) mg O₂*l⁻¹ and a modelled mean minimum of 5.8 (± 1.90) mg O₂*l⁻¹ at km 644. At these both sites about 16 % of the measured and modelled values were below 3.1 mg O₂*l⁻¹ and below 3.9 mg O₂*l⁻¹, respectively. Further downstream at the seaward limit of the freshwater region at km 660, the oxygen content is elevated. The measurements show a mean value of 8.0 mg O₂*l⁻¹ and the model results a value of 6.4 mg O₂*l⁻¹, i.e. the increase of the oxygen concentration in the model simulation is less pronounced.

Considering the variability of the daily measured oxygen content, the highest σ with 1.8 mg O₂*l⁻¹ appears at km 609 as well as in the oxygen minimum zone of the estuary at km 629. Concerning the model results, a σ value of 1.8 mg O₂*l⁻¹ is calculated for the reach from km 619 to km 647.

Oxygen budget of the estuary

The simulated oxygen consumption as well as input rates show clear longitudinal differences (Tab. 4). In the upstream section of the estuary at km 609, higher utilisation rates (consumption -1.72 and input $1.04 \text{ mg O}_2 \cdot \text{l}^{-1} \cdot \text{d}^{-1}$) are calculated than at the more downstream sections. Additionally at both upstream sites (km 609 and km 629) the gap between consumption and input is large (the delta of the absolute values of the summed input as well as consumption rates is 0.68 and $0.66 \text{ mg O}_2 \cdot \text{l}^{-1} \cdot \text{d}^{-1}$, respectively), while at the furthest downstream section (km 660) a balanced oxygen budget is calculated.

Concerning the single processes a strong longitudinal decrease of algal related processes is obvious: production rates of $1.11 \text{ mg O}_2 \cdot \text{l}^{-1} \cdot \text{d}^{-1}$ fall down to $0.03 \text{ mg O}_2 \cdot \text{l}^{-1} \cdot \text{d}^{-1}$ and the absolute values of the respiration rates from 0.87 down to $0.04 \text{ mg O}_2 \cdot \text{l}^{-1} \cdot \text{d}^{-1}$. By this the phytoplankton oxygen balance concerning input versus respiration turns from a positive value (delta $0.24 \text{ mg O}_2 \cdot \text{l}^{-1} \cdot \text{d}^{-1}$ at km 609) into a negative one (delta $-0.07 \text{ mg O}_2 \cdot \text{l}^{-1} \cdot \text{d}^{-1}$ and $-0.01 \text{ mg O}_2 \cdot \text{l}^{-1} \cdot \text{d}^{-1}$ at km 629 and 660), i.e., the algae respire more oxygen than they produce. The overall decrease of the rates is simply explained by the decrease of algal biomass, while the change in ratio is mainly due to stronger light limitation in the deeper sections of the estuary.

Table 4: Oxygen budget in the freshwater region of the Elbe Estuary – seasonal (May – October 2006) mean rates [$\text{mg O}_2 \cdot \text{l}^{-1} \cdot \text{d}^{-1}$] and standard deviation (in brackets) of processes and the sum of consumption and input rates at three different sites (km 609, km 629, km 660).

Processes	Seasonal mean rate [$\text{mg O}_2 \cdot \text{l}^{-1} \cdot \text{d}^{-1}$]		
	km 609	km 629	km 660
Re-aeration	$-0.07 (\pm 0.15)$	$0.18 (\pm 0.14)$	$0.28 (\pm 0.09)$
O ₂ -production by algae	$1.11 (\pm 0.51)$	$0.19 (\pm 0.17)$	$0.03 (\pm 0.06)$
Σ Input	1.04	0.38	0.31
Respiration by algae	$-0.87 (\pm 0.40)$	$-0.26 (\pm 0.21)$	$-0.04 (\pm 0.05)$
Nitrification	$-0.02 (\pm 0.02)$	$-0.16 (\pm 0.15)$	$-0.10 (\pm 0.04)$
Heterotrophic consumption	$-0.26 (\pm 0.08)$	$-0.30 (\pm 0.13)$	$-0.12 (\pm 0.05)$
Respiration by zooplankton	$-0.07 (\pm 0.06)$	$-0.18 (\pm 0.17)$	$-0.04 (\pm 0.04)$
Sediment oxygen demand	$-0.49 (\pm 0.08)$	$-0.12 (\pm 0.01)$	$-0.02 (\pm 0.006)$
Σ Consumption	-1.72	-1.04	-0.31

The physical re-aeration rate is strongly driven by the existing oxygen saturation. Therefore due to a mean oversaturation during the season at km 609 an export of oxygen is calculated. Downstream the atmospheric oxygen input is higher at km 660 than at km 629, which might be due to a lower mean depth at this site of the estuary. Regarding the heterotrophic consumption of oxygen, it is evident that it is the most important consumption process at the sites further downstream (km 629 and km 660).

At km 629 all other rates (nitrification, sediment oxygen demand and respiration by zooplankton) have a significant proportion on the overall consumption of oxygen as well. At km 660, additionally to the heterotrophic consumption, only the nitrification is an im-

portant consumption process. Concerning the most upstream site at km 609, the sediment oxygen demand shows higher rates than the heterotrophic oxygen consumption. The comparable low mean water depth (3.6 m) at this site supports the impact of the sediment on the oxygen budget of the water column.

4.3 Validation of the long term simulation of water quality parameters

Water temperature

The long term series of the period 1998 to 2010 of modelled water temperature (daily means) is illustrated for three sites (km 609, 629, 660) along the estuary and compared to daily means of water temperature derived from continuous measuring stations at these sites (Fig. 8).

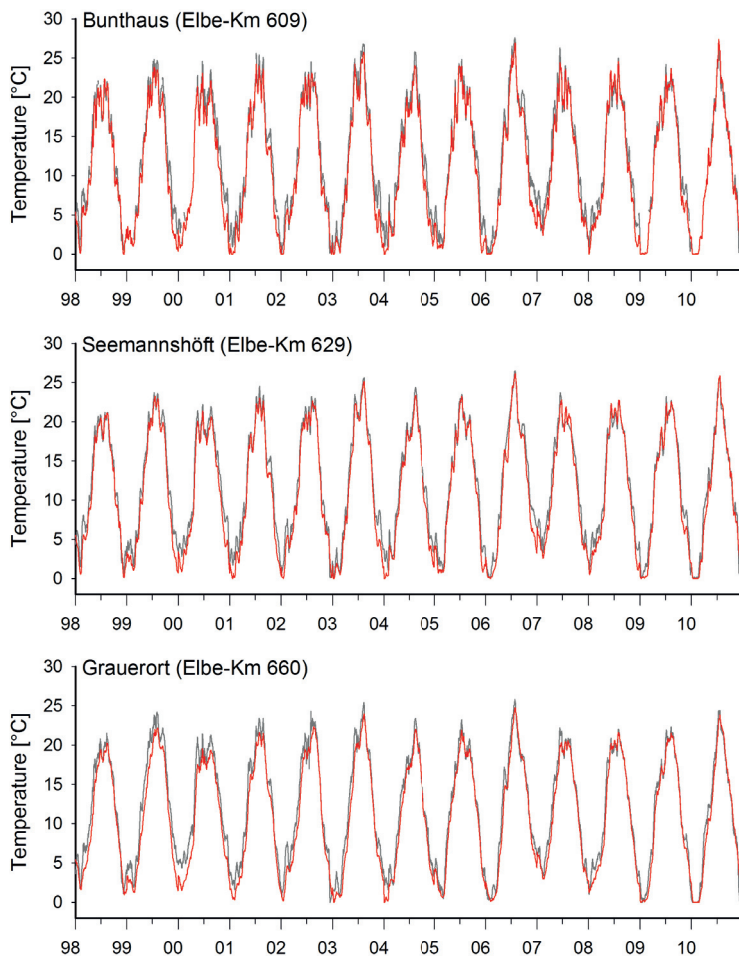


Figure 8: Measured (grey line) and modelled (red line) water temperature [°C] at Bunthaus (km 609), Seemannshöft (km 629) and Grauerort (km 660) for the years 1998-2010 (Measured data: Institute of Hygiene and Environment, Hamburg and NLWKN Stade).

The deviations are quantified by the calculation of the Nash-Sutcliffe Efficiency (NSE) (MORIASI et al. 2007). The NSE indicates the difference of a plot of measured and modelled data from a 1:1 plot. By using NSE it can be noticed that the modelled and measured values show a good agreement (the NSE based on daily data ranges between 0.960 and 0.967 at all sites) concerning the seasonal dynamics.

For the sites at km 609 and km 629 the compliance is weaker in winter (NSE: 0.888 and 0.944) than in summer, i.e., particularly during the vegetation period the modelled data fit the measured data well. The squared correlation coefficient (r^2) of measured and modelled values for all three sites range between $r^2 = 0.971$ and 0.976 . The corresponding slopes (s) of the linear correlation between $s = 0.931$ to 0.949 proof that the simulation slightly underestimates the water temperature. The seasonal differences between measured and modelled values can be explained by the lack of heat discharge from cooling plants, with the highest impact during winter time. Another reason for deviations between measurement and simulation is due to the 1d approach neglecting the effect of tidal flats on heat budget of the estuarine water body.

Chlorophyll

The algal biomass is continuously measured in the estuary at km 609 and km 629 by probes using the fluorescence-method. For comparison with the modelled chl_a values (Fig. 9), which are related to chl_a determined by German standard method using alcohol extraction and photometric measurement (see description of chl_a as a input parameter at the model boundaries), the fluorescence values are multiplied by factor 1.7.

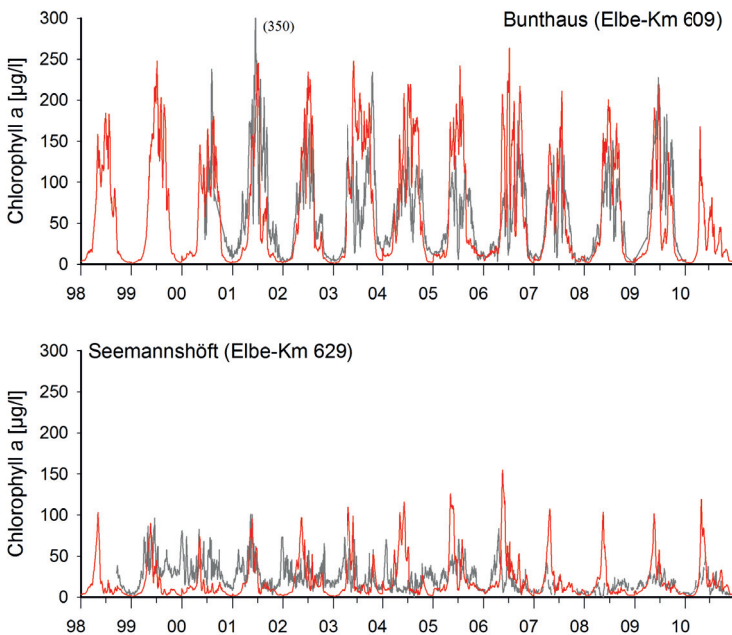


Figure 9: Measured (grey line) and modelled (red line) chlorophyll a [$\mu\text{g}\cdot\text{l}^{-1}$] at Bunthaus (km 609), Seemannshöft (km 629) and Grauerort (km 660) for the years 1998-2010 (Measured data: Institute of Hygiene and Environment, Hamburg).

For the period 2000 to 2009 the seasonal dynamics of chl_a at km 609 is adequately simulated for most of the years (NSE = 0.382), although for some distinct years, e.g. 2003 and 2006, an overestimation of chl_a by the simulation is visible. Using again the seasonal mean (May – October) for comparison a slightly higher mean of $108 (\pm 66) \mu\text{g chl}_a \cdot \text{l}^{-1}$ is calculated by the model in relation to the measured mean of $93 (\pm 51) \mu\text{g chl}_a \cdot \text{l}^{-1}$. Considering the modelled and measured values at km 629 for the period 1998 to 2010 seasonal differences are notably. In most of the years the simulated chl_a concentrations in spring and early summer overshoot the observations. Nevertheless, the seasonal mean of the simulated values ($28 \pm 27 \mu\text{g chl}_a \cdot \text{l}^{-1}$) is slightly lower than the measured one ($33 \pm 16 \mu\text{g chl}_a \cdot \text{l}^{-1}$). The seasonal differences are reflected in a low NSE of 0.007 for km 629.

Oxygen

For most of the sites along the estuary the modelled oxygen agrees well with the measurements (Fig. 10). The measured values are daily means calculated based on continuous measurements (each 5 min) with probes. The seasonal dynamics and especially the low oxygen contents in summer are well reproduced by the simulations. Concerning the whole period 1998 to 2010 the seasonal mean (May – October) of the oxygen content at km 609 is $9.6 \text{ mg O}_2 \cdot \text{l}^{-1}$ for the measurements and $10.3 \text{ mg O}_2 \cdot \text{l}^{-1}$ for the simulations, at km 629 5.7 and $6.9 \text{ mg O}_2 \cdot \text{l}^{-1}$, at km 635 6.4 and 6.2 , and at km 660 7.8 and $6.7 \text{ mg O}_2 \cdot \text{l}^{-1}$. The NSE reflects the good agreement between simulation and measurement for km 629 (NSE = 0.758), km 635 (NSE = 0.844) and km 660 (NSE = 0.725). However, the NSE for km 609 is lower (NSE = 0.284). These differences are confirmed by the squared correlation coefficient (r^2) of km 629 to 660, which range between $r^2 = 0.778$ and 0.857 , and a clearly lower r^2 of 0.296 at km 609. The corresponding slopes (s) show values above 1 for km 609 ($s = 1.016$) and km 629 ($s = 1.042$) meaning a slight overestimation of the modelled oxygen contents exists. At the more downstream stations the slopes fall below 1 (km 635 $s = 0.963$, km 660 $s = 0.936$) pointing to an underestimation of the simulated oxygen values.

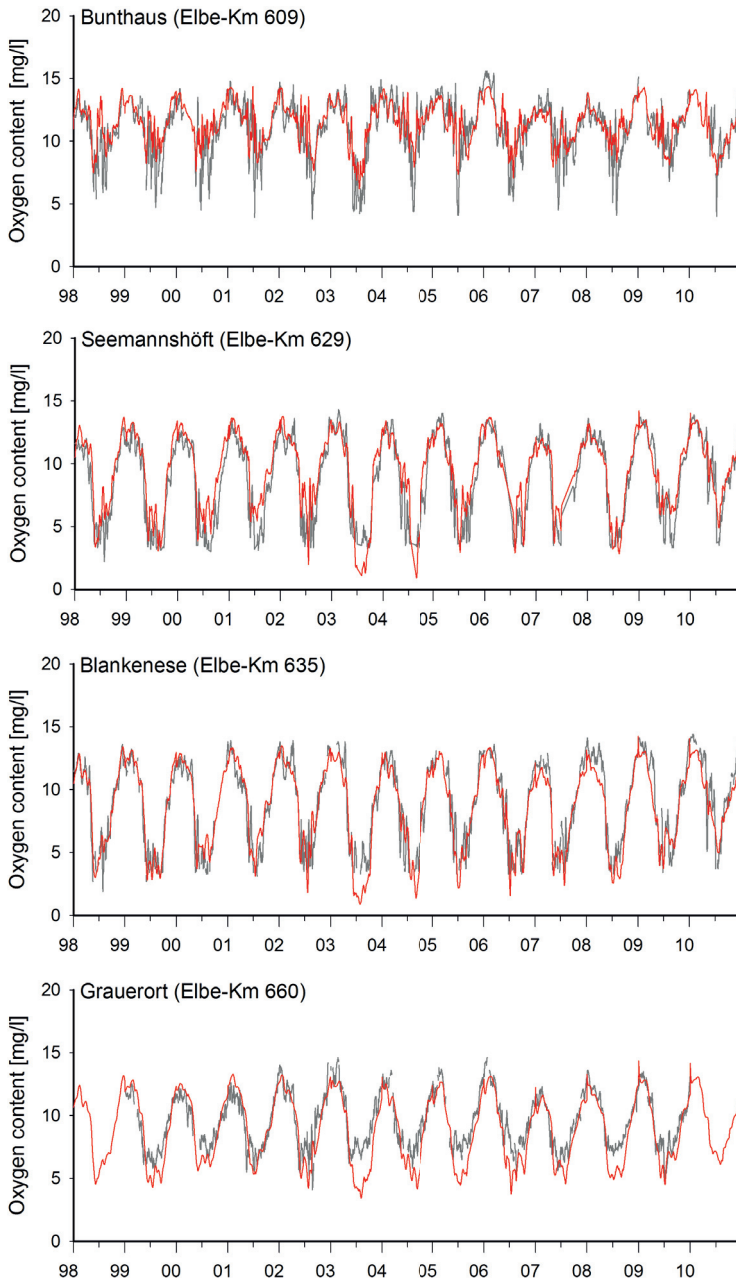


Figure 10: Measured (grey line) and modelled (red line) oxygen [$\text{mg}\cdot\text{l}^{-1}$] at Bunthaus (km 609), Seemannshöft (km 629), Blankenese (km 635) and Grauerort (km 660) for the years 1998-2010 (Measured data: Institute of Hygiene and Environment, Hamburg and NLWKN Stade).

4.4 Simulation of water temperature distribution in the Elbe Estuary with 2d QSim

The distribution of water temperature in the Elbe Estuary is simulated with a 2d approach of QSim coupled with the more-dimensional hydrodynamic model casu. The same meteorological forcing as in the 1d QSim model approach has been used. The upper model boundary is situated at the weir of Geesthacht (km 585) and is forced with the 1d model results for water temperature. For the 09/07/2010 the daily mean water temperature is higher in the side channel system and its tidal flats than in the main channel (Fig. 11). The measured and simulated daily means of water temperature in the main channel at buoy D1 (km 643) reached 23.62 and 23.35 °C and in the side channel at buoy HNE 24.41 and 24.09 °C, i.e. the difference between the main channel and the side channel is 0.79 and 0.74 °C respectively. The largest measured difference during the daily cycle in the main channel is 1.8 °C, while the simulated difference is lower with a value of 1.08 °C. Measured daily amplitude at buoy HNE is 3.4 °C and 1.7 °C for the simulation.

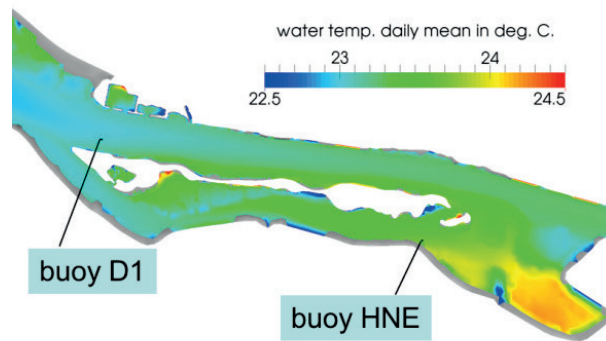


Figure 11: Distribution of daily mean water temperature [°C] on 09/07/2010 in the Elbe Estuary between km 636 and km 653 including the side channel Hahnöfer Nebenelbe and adjacent tidal flats.

Comparison of measurement and simulation of the water temperature for a ten day period from 03/07/2010 to 13/07/2010 shows that the overall level and range of temperature is sufficiently matched by the model results. Mean water temperature for measurements at buoy D1 is 23.41 °C and for simulations 23.06 °C, while at buoy HNE values of 24.41 and 24.03 °C were reached. Again the measured daily range of water temperature is higher than the simulated one. A mesh refinement is planned to reveal whether the transport modelling or the simulation of sediment heat balance is responsible for this effect.

5 Discussion

Water quality modelling is a very simplifying reproduction of the real world, mainly due to the necessary reduction of biological and functional diversity of ecosystems. For example, the phytoplankton community of the Elbe Estuary consists of more than 290 species (KOPPELMANN and KIES 1989 published in ARGE 1998), all with a species-specific

physiology. The water quality model QSim uses a common approach where only three functional algal groups (diatoms, green algae and cyanobacteria) with three sets of physiological parameters represent the whole community. Going deeper into detail, the model description of physiological processes is a simplification too, because separate processes often are combined or even neglected. Water flows (hydrodynamic) can be better reproduced in models, because water motion processes are more suitable for physical and mathematical descriptions.

A practical consequence of this difference in modelling simplification is the fact that many more calibration runs and re-runs of biogeochemical simulations are needed than for hydrodynamic simulations. This favours the approach of off-line coupling because of the advantage of saving hardware resources if only the biogeochemical simulations have to be run. By this approach, the computation of transport for a large number of variables, representing concentrations as well as process rates, for multiple long term water quality simulations becomes feasible.

We show the importance of large scale (catchment) water quality modelling for quantitative analysis of oxygen deficits in the freshwater region of the Elbe Estuary. Applying this approach, the importance of water residence times in each part of the system becomes obvious. There are comparably short retention times in the river (5-10 days), but elevated retention times in the tidally influenced estuary (weeks) depending on river discharges. Already in the freshwater region, including the deep section of Hamburg Harbour, retention times increase clearly. Water retention time changes are highly significantly at the scale of days, because this time scale is relevant for biological processes e.g. growth, decay or grazing (MONSEN et al. 2002).

A crucial point for modelling estuarine budgets and processes is the quality of the input signal from the river. The necessary data could be derived directly from measurements near the entrance of the river into the estuary, but seldom all of the needed parameters are measured in sufficient resolution, and therefore, no consistent set of parameters at the boundary is provided. Using input signals derived from measurements near the entrance of the estuary leads to another disadvantage concerning modelling that the modelled process rates of different modules are not immediately fully in agreement. To overcome these drawbacks we recommend a large scale approach and expanded the model area, including 585 km inland river stretch of the Elbe, although the focus remains on the oxygen budget of the estuary. Thereby, the modelling results in the estuary become less dependent on the boundary conditions and simulated model rates in the estuary become consistent.

In order to reflect biological seasonality, it is important to produce water quality simulations on a seasonal scale. For example, the yearly cycle of growth and decay of phytoplankton plays a major role to the oxygen budget of the estuary. Further on, even longer time spans are needed to evaluate the interannual variability of water quality for management purposes.

Based on the 1d approach, the requirements for long term modelling of water quality in the context of climate change research can be fulfilled. The results for the 13-year period (1998-2010) of the heat and the oxygen budget of the Elbe could be used as a reference period for studying impact of climatically changed air temperature or discharges. This approach is realized in the KLIWAS research program (BFG et al. 2014). The results show that in future scenarios the change of discharge conditions is the major influencing

factor on the algal development in the river section of the Elbe and on the resulting oxygen budget of its estuary (QUIEL et al. 2011, HEIN et al. 2014).

In the second section, we discuss the results concerning the modelling of phytoplankton and oxygen budget in the Elbe river/estuary system. The high importance of the river discharge and thereby riverine load of algal derived organic carbon is a very noticeable feature of the Elbe Estuary. This is less true for estuaries of rivers with a smaller catchment or in more arid areas of the world. These systems are more characterised by marine inflow or autochthonous primary production (COLE and PEIERLS 1992). In the case of the Elbe Estuary, the influence of the river load is restricted to the freshwater region, a very expanded zone in this estuary. Due to high importance of the riverine load, we simulate higher rates of microbial activity in the upper region of the estuary than more downstream sections of the Elbe Estuary. The longitudinal decrease of measured BOD₇-values in the estuary reflects the decline of microbial activity, with the lowest level of activity from the lower end of the freshwater zone until the mesohaline zone (km 660 and km 725), including the turbidity zone.

Our results confirm that only by a satisfying modelling of growth of phytoplankton in the eutrophic river section of the Elbe, the oxygen budget of the estuary can be analysed. In eutrophic rivers like the Elbe, phytoplankton is the main driver of organic carbon cycling and therefore providing carbon substrate for heterotrophic oxygen consumption by bacteria (THORP and DELONG, 2002). In addition, the phytoplankton directly produces or respire oxygen. In the freshwater region of the Elbe Estuary the direct impact of phytoplankton on the oxygen budget switches from a positive one (km 585 to km 609) – mean production is higher than respiration – to a negative one in the more downstream section of the estuary between km 609 and 629. Along this stretch, the water depth increases clearly and algae growth becomes light limited, while the respiration of the existing biomass is still high.

Looking at the fate of phytoplankton, a challenge for understanding and modelling is the disappearance of the algal biomass in the upper freshwater section of the Elbe Estuary. Physiological die-off, sedimentation or grazing are important internal and external loss processes, respectively (MORTAZAVI et al. 2000, HAGY III et al. 2005). The physiological die-off needed some time before algal biomasses disappeared, although a nutrient limitation may support the waning of the algae. In well mixed estuaries like the Elbe sedimentation needs areas of low flow velocities or a long lasting slack water period for an effective impact on the reduction of algal biomass. The influence of harbour basins in the Hamburg area may fulfil the above mentioned criteria and should be a subject for application of more dimensional modelling.

Our 1d modelling approach identifies grazing as the dominant loss process for phytoplankton in the Elbe Estuary. Seasonal mean high grazing rates of 0.5 per day mean that nearly 40 % of the standing stock of the phytoplankton is reduced per day. Calculated maximal grazing rates of 2.0 per day lead to a loss of 87 % and by that a nearly complete control of the algal biomass. In the Schelde estuary such high grazing pressure mainly by microzooplankton is described and community grazing rates of 0.41 to 1.83 per day were measured (LIONARD et al. 1997). The Elbe Estuary is a favourable habitat for estuarine copepods and for river borne rotifers, mainly due to the sufficient food supply. Already in the river, strong increases of zooplankton abundances were observed during longitudinal surveys from Schmilka to the weir of Geesthacht (HOLST 2006, HARDENBICKER

2014). The maximum reported abundances were reached at Geesthacht with up to 10,000 Ind* l^{-1} for the dominant zooplankton group of rotifers and up to 40 Ind* l^{-1} for crustaceans (HOLST 2006). Our modelling results for the year 2006 show a seasonal mean of 320 (+/- 190) rotifers of Ind* l^{-1} at the entrance to the estuary at km 586.

In the estuary, the zooplankton abundances reached a maximum of 4,250 Ind* l^{-1} at km 629 and a seasonal mean of 1,500 Ind* l^{-1} . The counted seasonal mean zooplankton (rotifers and crustaceans) abundances at that site were 1,050 Ind* l^{-1} . Comparable high abundances between 200 and 1800 Ind* l^{-1} were reported for the Schelde estuary (LIONARD et al. 1997). One explanation of the difference between modelled and observed abundances in the Elbe might be due to the fact that the zooplankton in the estuary is not longer represented by the rotifers as assumed in the QSim model approach, but copepods with higher biovolume and individual dry weight become the dominant group. Secondly, higher zooplankton abundances are simulated, because no external loss of zooplankton to a higher trophic level of the food web is taken into account. However, it is known that zooplankton is an important prey for fish larvae and juvenile fishes in estuaries (MEHNER and THIEL 1999) and abundances could be reduced clearly by feeding. Many further investigations and data are required to model and evaluate the role of zooplankton in the Elbe Estuary.

In addition to the longitudinal development of phytoplankton and oxygen, the lateral distribution of the oxygen concentrations is of scientific and management concerns. The importance of tidal flats, side channel systems or harbour basins as sinks or sources for oxygen are important issues which can only be studied in detail by applying a more dimensional model approach. As a first step we proof our coupling concept by simulating the heat budget of a side channel system, showing notable differences of water temperature between main channel and side channel. Higher water temperatures in the side channel are due to lower mean water depth and the warming effect by tidal flats.

6 Conclusions and outlook

The 1d QSim simulation approach confirms that the growth and decline of phytoplankton in the eutrophic Elbe and its estuary has to be simulated accurately to get a realistic picture of the oxygen budget of the estuary. In the eutrophic river phytoplankton biomass is produced up to a seasonal mean (May-October 2006) of nearly 150 $\mu\text{g chl}a \cdot l^{-1}$. In the freshwater region of the estuary algae growth becomes negative due to light limitation, leading to net oxygen consumption by algae due to respiration. Additionally, high grazing losses by zooplankton (seasonal mean of 0.5 per day) reduces algal biomass drastically. Algal derived organic carbon imported from the river and originated in the estuary during algal die-off provides the substrate for heterotrophic oxygen consumption by bacteria.

The large scale 1d QSim approach including a 585 km long river section provides a consistent set of water quality parameter as an input signal for modelling the oxygen budget of the Elbe Estuary. Furthermore, the ability of simulating large time periods which is a crucial need for climate change modelling of water temperature and oxygen has been proofed. In contrast, for detailed studies in the side channel systems of the Elbe Estuary with the tidal flats the higher resolution of the more dimensional model is shown to be essential. Such horizontal differences of water quality parameters mainly caused by

morphological structures as side channels or harbour basins are of ecological importance (improved oxygen conditions or feeding habitat for young fish) and should be subject of more dimensional modelling in estuaries. Even so more realistic modelling of water residence times in certain domains of the estuary based on more dimensional modelling is required.

7 Acknowledgements

We are grateful to Werner Blohm, Carsten Viergutz and Helmut Fischer for support and constructive remarks on the manuscript. The results shown here are based on the results of project 3.08 „Climate change related impacts on the oxygen budget of North Sea estuaries due to alterations of river discharge and nutrient and carbon load – potential adaptation strategies for sediment management“ of the research program KLIWAS financed by the Federal Ministry of Transport and Digital Infrastructure (BMVI).

8 References

- ARGE ELBE: Gewässerökologische Studie der Elbe. 98 pp., 1984.
- ARNDT, S.; LACROIX, G.; GYPENS, N.; REGNIER, P. and LANCELOT, C.: Nutrient dynamics and phytoplankton development along an estuary-coastal zone continuum: A model study. *Journal of Marine Systems*, Vol. 84, 3-4, 49-66, 2011.
- BECKER, A.; KIRCHESCH, V.; BAUMERT, H.Z.; FISCHER, H. and SCHÖL, A.: Modelling the effects of thermal stratification on the oxygen budget of an impounded river. *River Research and Applications*, Vol. 26, 5, 572-588, 2010.
- BERGEMANN, M.; BLÖCKER, G.; HARMS, H.; KERNER, M.; MEYER-NEHLS, R.; PETERSEN, W. and SCHRÖDER, F.: Der Sauerstoffhaushalt der Tideelbe. *Die Küste*, Vol. 58, 199-261, 1996.
- BERGFELD, T.: Dynamics of microbial food web components in three large rivers (Rhine, Mosel and Saar) with the main focus on heterotrophic nanoflagellates. Thesis. University Cologne, 126 pp., 2002.
- BFG: Das Gewässergütemodell QSim: Handbuch zur Benutzeroberfläche GERRIS. Report No. 1778, 99 pp., 2013.
- BFG; DWD; BSH and BAW: KLIWAS Auswirkungen des Klimawandels auf Wasserstraßen und Schifffahrt - Entwicklung von Anpassungsoptionen. Synthesebericht für Entscheidungsträger, KLIWAS-57/2014, 2014.
- BILLEN, G.: Protein degradation in aquatic environments. In: CHRÖST, R. (Ed.): *Microbial enzymes in aquatic environments*. Springer Verlag, New York, 122-142, 1991.
- BILLEN, G.; GARNIER, J.; FICHT, A. and CUN, C.: Modelling the Response of Water Quality in the Seine River Estuary to Human Activity in its Watershed Over the Last 50 Years. *Estuaries*, Vol. 24, 6B, 977-993, 2001.
- BRUCE, L.C.; COOK, P.L.M.; TEAKLE, I. and HIPSEY, M.R.: Controls on oxygen dynamics in a riverine salt-wedge estuary – a three-dimensional model of the Yarra River estuary, Australia. *Hydrol. Earth Syst. Sci. Discuss.*, Vol. 10, 9799-9845, 2013.
- CASPER, H.: Die Sauerstoffproduktion einer Bucht im Süßwasserbereich des Elbe-Ästuars. – Untersuchungen im „Mühlenberger Loch“ in Hamburg. *Archiv für Hydrobiologie, Suppl.-Bd. 62, 5, 509-542, 1984.*

- CASULLI, V. and CHENG, R.T.: Semi-implicit finite difference methods for three-dimensional shallow water flow, *International Journal for Numerical Methods in Fluids*, Vol. 15, 629-648, 1992.
- CUNGE, J.A.; HOLLY, F.M. and VERWEY, A.: *Practical Aspects of Computational River Hydraulics*. Pitman Advanced Publishing Program, London, 420 pp., 1980.
- CERCO, C.F. and COLE, T.: Three-dimensional eutrophication model of Chesapeake Bay. *Journal of Environmental Engineering*, Vol. 119, No. 6, 1006-1025, 1993.
- COLE, J.J. and PEIERLS, P.L.: Can phytoplankton maintain a positive carbon balance in a turbid, freshwater, tidal estuary? *Limnol. Oceanogr.*, 37, 1608-1617, 1992.
- DI TORO, D.M.: *Sediment flux modelling*. Vol. 116. Wiley, New York, 624 pp., 2001
- DUCHARNE, A.; BAUBION, C.; BEAUDOIN, N.; BENOIT, M.; BILLEN, G.; BRISSON, N.; GARNIER, J.; KIEKEN, H.; LEBONVALLET, S.; LEDOUX, E.; MARY, B.; MIGNOLET, C.; POUX, X.; SAUBOUA, E.; SCHOTT, C.; THÉRY, S. and VIENNOT, P.: Long term prospective of the Seine River system: Confronting climatic and direct anthropogenic changes. *Science of the Total Environment*, Vol. 375, 292-311, 2007.
- FLÜGGE, G.: *Gewässerökologische Überwachung der Elbe*. Abh. Naturw. Ver. Bremen, 40, 217-232, 1985.
- FRJASINOV, I.V.: Algoritm resenija raznostnyh zadac na grafah. *Zyurnal vycislitel'noj matematiki i matematiceskoj fiziki* 10, 1970.
- GARNIER, J.; SERVAIS, P.; BILLEN, G.; AKOPIAN, M. and BRION, N.: Lower Seine River and Estuary (France) Carbon and Oxygen Budgets During Low Flow. *Estuaries*, Vol. 24, 6B, 964-976, 2001.
- GYPENS, N.; DELHEZ, E.; VANHOUTTE-BRUNIER, A.; BURTON, S.; THIEU, V.; PASSY, P.; LIU, Y.; CALLENS, J.; ROUSSEAU, V. and LANCELOT, C.: Modelling phytoplankton succession and nutrient transfer along the Scheldt estuary (Belgium, The Netherlands). *Journal of Marine Systems*, Vol. 128, 89-105, 2013.
- HAGY III, J.D., BOYNTON, W.R. and JASINSKI, D.A.: Modelling phytoplankton deposition to Chesapeake Bay sediments during winter–spring: interannual variability in relation to river flow. *Estuarine, Coastal and Shelf Science*, Vol. 62, 25-40, 2005.
- HARDENBICKER, P.: *Phytoplankton dynamics in two large rivers: long-term trends, longitudinal dynamics and potential impacts of climate change*. Thesis, Technical University of Dresden, 119 pp., 2014.
- HEIN, B.; WYRWA, J.; VIERGUTZ, C. and SCHÖL, A.: Projektionen für den Sauerstoffhaushalt des Elbe-Ästuars – Folgen für die Sedimentbewirtschaftung und das ökologische Potenzial. *Schlussbericht KLIWAS-Projekt 3.08*. KLIWAS-42/2014, doi: 10.5675/Kliwas_42/2014_3.08, 2014.
- HOLST H.: Zooplankton im Pelagial des Hauptstroms. In: PUSCH, M. and FISCHER, H. (Eds.): *Stoffdynamik und Habitatstruktur in der Elbe – Konzepte für die nachhaltige Entwicklung einer Flusslandschaft*. Weißensee Verlag, Berlin, 56-64, 2006.
- HOWARTH, R.; CHAN, F.; CONLEY, D.J.; GARNIER J.; DONEY S.C.; MARINO, R. and BILLEN, G.: Coupled biogeochemical cycles: Eutrophication and hypoxia in temperate estuaries and coastal marine ecosystems. *Frontiers in Ecology and the Environment*, Vol. 9, 1, 18-26, doi: 10.1890/100008, 2011.
- IKSR: Estimation of the effects of climate change scenarios on future Rhine water temperature development – Extensive Version. *International Commission for the Protection of the Rhine*. Report, 214, 57 pp., 2013.

- KIRCHESCH, V. and SCHÖL, A.: Das Gewässergütemodell QSim - Ein Instrument zur Simulation und Prognose des Stoffhaushaltes und der Planktodynamik von Fließgewässern. *Hydrologie und Wasserbewirtschaftung*, Vol. 43, 302-309, 1999.
- LEONARD, B.P.: A stable and accurate convective modelling procedure based on quadratic upstream interpolation. *Computer Methods in Applied Mechanics and Engineering*, Vol. 19, 59-98, 1961.
- LIONARD, M.; AZEMAR, F.; BOULETREAU, S.; MUYLEAERT, K.; TACKX, M. and VYVERMAN, W.: Grazing by meso- and microzooplankton on phytoplankton in the upper reaches of the Schelde estuary (Belgium/The Netherlands). *Estuarine, Coastal and Shelf Science*, Vol. 64, 764-774, 2005.
- MATZINGER, A.; FISCHER, H. and SCHMID, M.: Modellierung von biogeochemischen Prozessen in Fließgewässern. *Handbuch Angewandte Limnologie*, 29, 5/12, 32 pp., 2012.
- MORIASI, D.N.; ARNOLD, J.G.; VAN LIEW, M.W.; BINGNER, R.L.; HARMEI, R.D. and VEITH, T.L.: Model evaluation guidelines for systematic quantification of accuracy in watershed simulations. *Transactions of the American Society of Agricultural and Biological Engineers*, Vol. 50, 885-900, 2007.
- MEHNER, T. and THIEL, R.: A review of predation impact by 0+ fish on zooplankton in fresh and brackish waters of the temperate northern hemisphere. *Environmental Biology of Fishes*, Vol. 6, 169-181, 1999.
- MONSEN, N.E.; CLOERN, J.E.; LUCAS, L.V. and MONISMITH, S.G.: A comment on the use of flushing time, residence time, and age as transport time scales. *Limnology and Oceanography*, Vol. 47, 5, 1545-1553, 2002.
- MORTAZAVI, B.; IVERSON, R.L.; LANDING, W.M.; LEWIS, F.G. and WENRUI, H.: Control of phytoplankton production and biomass in a river-dominated estuary: Apalachicola Bay, Florida, USA. *Mar. Ecol. Prog. Ser.*, Vol. 198, 19-31, 2000.
- OLLINGER, D.: Modellierung von Temperatur, Turbulenz und Algenwachstum mit einem gekoppelten physikalisch-biologischen Modell. Thesis, Universität Heidelberg, 1999.
- OPPERMANN, R.: Eindimensionale Simulation allmählich veränderlicher instationärer Fließvorgänge in Gewässernetzen. *Mitteilungen des Instituts für Wasserwirtschaft*, H. 50. VEB Verlag für Bauwesen, Berlin, 1989.
- OPPERMANN, R.: Das Programmsystem HYDRAX 5.0 – Mathematisches Modell und Datenschnittstellen. *Ingenieurbüro für Wasser und Umwelt Berlin*, 11 pp., 2010.
- PAERL, H. and PINCKNEY, J.: Ecosystem response to interannual and watershed organic matter loading: consequences for hypoxia in the eutrophying Neuse River Estuary, North Carolina, USA. *Marine Progress Series*, Vol. 146, 17-25, 1998.
- PUSCH, M.; ANDERSEN, H.E.; BÄTJE, J.; BEHRENDT, H.; FISCHER, H.; FRIBERG, N.; GANCARCZYK, A.; HOFFMANN, C.C.; HACHOL, J.; KRONVANG, B.; NOWACKI, F.; PEDERSON, M.L.; SANDIN, L.; SCHÖLL, F.; SCHOLTEN, M.; STENDERA, S.; SVENDSEN, L.M.; WNUK-GLAWDEL, E. and WOLTER, C.: Rivers of the Central European Highlands and Plains. In: TOCKNER, K.; ROBINSON, C.T. and UEHLINGER, U. (Eds.): *Rivers of Europe*. London, 525-576, 2009.
- QUIEL, K.; BECKER, A.; KIRCHESCH, V.; SCHÖL, A. and FISCHER, H.: Influence of global change on phytoplankton and nutrient cycling in the Elbe River. *Regional Environmental Change*, Vol. 11, 2, 405-421, 2011.
- RABALAIS, N.N.; EUGENE, R.; DIAZ, R.J. and JUSTIĆ, D.: Global change and eutrophication of coastal waters. *ICES Journal of Marine Science*, Vol. 66, 1528-1537, 2009.

- SALMASO, N. and BRAIONI, M.G.: Factors controlling the seasonal development and distribution of the phytoplankton community in the lowland course of a large river in Northern Italy (River Adige). *Aquatic Ecology*, Vol. 42, 533-545, 2008.
- SCHÖL, A.; EIDNER, R.; BÖHME, M. and KIRCHESCH, V.: Integrierte Modellierung der Wasserbeschaffenheit mit QSim. In: PUSCH, M. and FISCHER, H. (Eds.): *Stoffdynamik und Habitatstruktur in der Elbe*, Bd. 5., Weißensee Verlag, Berlin, 233-242, 2006a.
- SCHÖL, A.; EIDNER, R.; BÖHME, M. and KIRCHESCH, V.: Einfluss der Bühnenfelder auf die Wasserbeschaffenheit der Mittleren Elbe. In: PUSCH, M. and FISCHER, H. (Eds.): *Stoffdynamik und Habitatstruktur in der Elbe*, Bd. 5., Weißensee Verlag, Berlin, 243-263, 2006b.
- SCHÖL, A.; KIRCHESCH, V.; BERGFELD, T.; SCHÖLL, F.; BORCHERDING, J. and MÜLLER, D.: Modelling the chlorophyll *a* content of the River Rhine - Interrelation between riverine algal production and population biomass of grazers, rotifers and the zebra mussel, *Dreissena polymorpha*. *Internat. Rev. Hydrobiol.*, Vol. 87, 295-317, 2002.
- THORP, J.M. and DELONG, M.D.: Dominance of autochthonous autotrophic carbon in food webs of heterotrophic rivers. *Oikos*, Vol. 96, 3, 543-550, 2002.
- WYRWA, J.: Turbulenzmodellierung für stabil dichtegeschichtete Strömungen bei der Simulation des Transports von kohäsiven Sedimenten in Ästuaren. Thesis. TU Berlin, 2003.
- YASSERI, M.S.: Untersuchungen zum Einfluss von Sauerstoffmangelsituationen auf den mikrobiell-heterotrophen Stoffumsatz an Schwebstoffen in der Tideelbe. Adfontes-Verlag, Hamburg, 97 pp., 1999.
- ZHENG, L.; CHEN, C. and ZHANG, F.: Development of water quality model in the Satilla River Estuary, Georgia. *Ecological Modelling*, Vol. 178, 457-482, 2004.
- ZHU, Z.-Y.; ZHANG, J.; WU, Y.; ZHANG, Y.-Y.; LIN, J. and LIU, S.M.: Hypoxia of the Changjiang (Yangtze River) Estuary: Oxygen depletion and organic matter decomposition. *Marine Chemistry*, Vol. 125, 108-116, 2011.